Gamma-Ray Spectroscopy: Meteorite Samples And the Search for ^{98}Tc

by Kristopher L. Merolla

Physics Department
California Polytechnic State University
San Luis Obispo, California

February 2010

Approval Page

Title:	Gamma-Ray Spectroscopy: Meteorite Samples And the Search for ^{98}Tc
Author:	Kristopher L. Merolla
Date Submitted:	February 17, 2010

_____ _____

Senior Project Advisor Signature

0.0.0 Table of Contents

1.0.0 Introduction 4

1.1.0 A Method of Formation of Technetium 5

1.2.0 Acknowledgements 6

2.0.0 Procedures 7

2.1.0 The Spectrometer 7

2.1.1 Handling the Sample 7

2.1.2 Calibration 7

2.2.0 How To: Measuring Gamma Rays 8

2.2.1 Correction of Predicted Channels 8

2.2.2 Energy from Channel Determination 9

3.0.0 Data 10

3.1.0 Explaining the Tables 10

3.2.0 Tables 12

4.0.0 Analysis 15

4.1.0 Visual Aids 15

4.2.0 Peak Energies 16

4.3.0 Conversion of Peaks Found to MeV 17

5.0.0 Conclusion 18

6.0.0 Bibliography 19

0.0.1 List of Figures

Figure 1-1:	Decay scheme for ^{98}Tc	5
Figure 4-1:	3-D Peak Representation	15
Figure 4-2:	3-D Peak Representation (Mirrored Peaks)	16

0.0.2 List of Tables

Table 3-1:	Counts vs. Channel	12
Table 3-2:	Uncertainty of Counts	12
Table 3-3:	Mirror Image Spectra	13
Table 3-4:	Uncertainty for Mirror Image Spectra	13
Table 3-5:	Center Counts with Uncertainties Factored Out	14
Table 3-6:	Center Counts with Uncertainties Factored Out (Mirrored)	14
Table 3-7:	Summary of Results	14
Table 5-1:	Peak Energies Summary	18

0.0.3 List of Equations

Eqn. 1:	Channel to Energy Relationship	8
Eqn. 2:	Lower Detector Channel Correction	9
Eqn. 3:	Upper Detector Channel Correction	9
Eqn. 4:	Upper Detector Channel-Energy Relationship	9
Eqn. 5:	Lower Detector Channel-Energy Relationship	9
Eqn. 6:	Upper Detector Energy-Channel Conversion	10
Eqn. 7:	Lower Detector Energy-Channel Conversion	10
Eqn. 8:	Peak Channel Equation	10

1.0.0 Introduction

The focus of this project is low-count-level gamma-ray spectroscopy on meteorite samples in search of a particular isotope of Technetium (^{98}Tc), which according to stellar theory, should be present in the universe. The spectral lines for ^{99}Tc have, however, been observed in S-, M-, and N- type stars, which makes finding ^{98}Tc created naturally a possibility, and thus a search can be justified.

Technetium-98 has a half-life of about 4.2×10^6 years (4,200,000 years) and is created only artificially on Earth, so we expect that the meteorite samples would not be contaminated by ^{98}Tc from a source on Earth. Other isotopes do have similar decays as the ^{98}Tc which we are looking for, so careful examination of the data will need to be performed to rule out other possibilities if peaks are found in the correct areas. The meteorite used for this sample was a stony-iron meteorite, originally found at Lake Labyrinth, Australia in 1924.

Since the half-life of ^{98}Tc is relatively long compared to the time which we have to measure the decays, the length required for a useable run must be fairly long in order to detect an above background level of counts from our sample. Our sample was run for 50000 minutes (approximately 35 days), which we deemed sufficient to detect any ^{98}Tc that may be in the meteorite sample. The gamma-ray energies of interest for identifying ^{98}Tc are 0.6524 MeV and 0.7454 MeV, and so the gain and number of channels were set up such that the spectrometer readout would include these energies.

In order to look for these low level gamma-ray emissions, a two-dimensional anti-coincidence shielded gamma-ray spectrometer was used. This spectrometer was constructed by Dr. Roger Grismore, who is also the advisor for the project. The way that the spectrometer works is by using two scintillator detectors set 180 degrees from each other with a scintillating annulus surrounding them.

Coincident events are then recorded on a two-dimensional plot with the lower detector and upper detector energies each on their own axis, with a line of symmetry between the two. Single events are also recorded on two one-dimensional spectra. The annulus ring detector is set to anti-coincidence, which filters out gamma rays not originating from the sample chamber inside the detector, and so we expect the coincident

rays detected to be emitted only from the sample and not from any type of outside source, or from any internal Compton scattering.

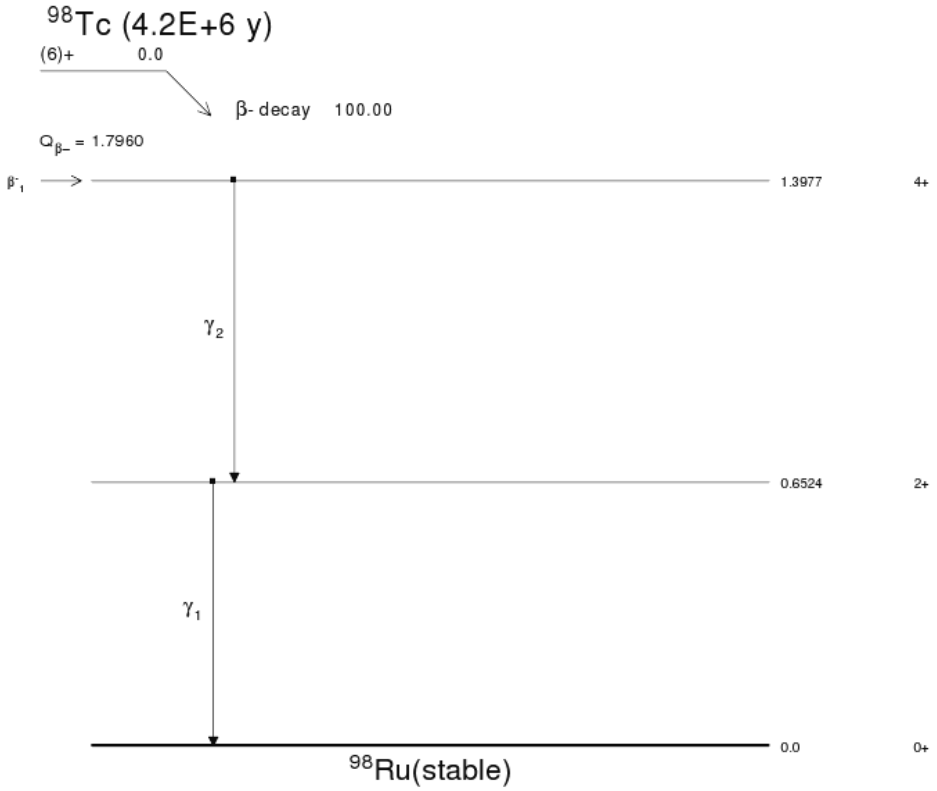

Figure 1-1. Decay scheme for ^{98}Tc

The decay emitting the 0.6524 MeV gamma ray and the decay emitting the 0.7454 MeV gamma ray are seen in coincidence. This will be useful for later reducing of our data and deciding whether or not we are looking at ^{98}Tc or some other isotope.

1.1.0 A Method of Formation of Technetium

One possible method for the formation of Technetium naturally has been explored by Robert Malaney in an article from Nature titled "Production of technetium in red giants by gamma-ray-induced fission." This article goes over various mathematical proofs for the energy needed to create Technetium as the fission yield from heavy isotopes. The radioactive chain that leads to the production of ^{99}Tc is shown in this article (with half lives in parenthesis) as:

$$\rightarrow {}^{99}\text{Zr}(35\text{s}) \rightarrow {}^{99}\text{Nb}(2.4\text{min}) \rightarrow {}^{99}\text{Mo}(67\text{h}) \rightarrow {}^{99}\text{Tc}(2.1\text{x}10^{5}\text{yr})$$

The article describes the formation of Technetium as a result of γ-ray-induced fission of the heavy nuclei in the hydrogen burning shell of red giants. Red giant stars are large in radii and sometimes massive, ranging from $0.5M_{\odot}$ to $6M_{\odot}$ with radii sometimes tens or hundreds of times larger than that of our Sun. These stars have exhausted the hydrogen that they used to burn inside their cores and now (as red giant stars) fuse hydrogen in a shell outside their core, which is where the fission we are talking about would take place. It is the energies of these gamma rays coming from the fusion of hydrogen in this shell that gives the energy needed to produce the Technetium which has been seen from the spectra of these stars. The radio isotope which we are looking for, ^{98}Tc, can be produced by (p,d) or (d,t) reactions on ^{99}Tc, all of which would be possible in red giant stars.

1.2.0 Acknowledgements

I would first, of course, like to acknowledge the invaluable direction of Dr. Roger Grismore, without whose help this study would not have been conducted, and for his dedication and knowledge in and of the field of spectroscopy. I would like to thank Dr. Grismore and Cal Poly for allowing me the opportunity to both work with an experienced research professor on a one on one basis, as well as perform work relative to my field of interest.

2.0.0 Procedures

2.1.0 The Spectrometer

The spectrometer is a very sophisticated machine and therefore must be used in a specific manner which preserves the integrity of the instrument, as well as of the samples inside the chamber.

2.1.1 Handling the Sample

The meteorite sample is always handled with great care to ensure both the integrity of the sample is intact, and that one is careful not to cross contaminate the sample with something from Earth. In order to do that, we take the following steps to ensure the sample is well managed.

1) Always wear a pair of latex gloves when handling the sample, never touch the meteorite with your bare hands. This will help ensure that no cross contamination of any type gets on the sample.
2) Change gloves often when handling different samples or any time you touch anything new. This again helps to ensure the sample is not contaminated with any outside sources. This is especially crucial when putting in and taking back out the calibration sources from the spectrometer.
3) Wearing long sleeve shirts (or in my case having a lab coat on) will help reduce the likelihood of dust or skin particles from getting inside the spectrometer housing and possibly contaminating a run.
4) Dual Ziploc bags are used around the sample to further keep outside influences from contaminating the sample.
5) The meteorite sample sits on a small cardboard stand inside the spectrometer for runs.

2.1.2 Calibration

Because individual runs of the spectrometer are so lengthy, it is necessary to calibrate the system every time we wish to make a run, whether it is a background run or a sample run. Calibration is important because it ensures that the channels which the events of decay are recorded correspond to the proper energy levels. To do this, we make

runs with a ^{137}Cs + ^{60}Co source, from which we know the energy of decay peaks as well as the channels we wish them to go in. From ^{137}Cs we know there will be a decay with an energy of 0.6616 MeV, which we want to be in channel 132.3 of the detector. From the ^{60}Co source we expect to see two decay energies of 1.1732 MeV and 1.3325 MeV, which we desire in the channels 234.6 and 266.5, respectively.

With the energies of the target calibration source known, 7 minute runs are made and the corresponding adjustments to gains and baselines are carefully made on the spectrometer. After a calibration run has completed, a program on the computer is used to determine the location of the characteristic peaks for the gamma rays discussed above. The name of the program that does this is CALDSK.exe. The tolerances (given by this program on a printout) for a properly calibrated spectrometer are: baselines to be 0.0 ± 0.1 and the sum gain of the ^{60}Co peaks to be 501.1 ± 1.0. Adjustments are made after each calibration run, and a new 7 minute calibration run is made until these values are reached. Once the spectrometer has been successfully calibrated, we can begin a sample run with confidence that our channels are properly calibrated.

2.2.0 How To: Measuring Gamma Rays

Since the goal of the procedure is to determine an energy level for an event, we need to determine the energy from what we are given by the program running the spectrometer. Lower energy levels are in the lower channel number cells, and higher energy levels are in the higher channel number cells, as you would expect. Since output from the spectrometer gives a count and channel numbers, we need a method for converting these channel numbers into something that we can use like energy levels.

2.2.1 Correction of Predicted Channels

The relationship between the channel number and the energy of that channel used to plot data points from the spectrometer comes from the linear relationship:

$$\text{Channel \#} = \text{Gain}*\text{Energy} + \text{Baseline} \quad (1)$$

Where Gain refers to the gain of the amplifiers, Energy refers to the energy of the decay, and Baseline refers to a linear offset. (*The gain is determined by the needs of the experiment and is set before a run.*)

There is also a correction that needs to be made for both the lower and the upper detectors for the predicted channel numbers. This correction is determined with known energy emissions (using a sample source), and for the lower detector the correction is linear:

$$\text{Correction (\# of channels)} = 0.5509 - 0.1387 * x \quad (2)$$

And for the upper detector, we have a second degree relationship:

$$\text{Correction} = 0.3539 + 0.001804 * x + 0.3645 * x^2 \quad (3)$$

The x term in both equations represents the energy that we are looking for in MeV. These relationships will be useful for the analysis of our data, and help to determine what channels we need to look at for our 0.6524 MeV and 0.7454 MeV gamma ray emissions.

2.2.2 Energy from Channel Determination

In order to go from channels to energies (in MeV) we need a way to know what energies lie in each channel. This is done simply for each sample spectrum by observing certain peaks which always appear in the singles spectra along the edges of the two-dimensional main spectrum. These peaks at gamma-ray energies of 0.511 MeV, 1.461 MeV, and 2.223 MeV. After each sample run, the channels of these strong peaks are noted by the computer software and recorded for the upper and lower detectors. Peak channels (in ascending order of energies listed above) are for the run which I analyzed:

UPPER	24.06	71.79	109.68
LOWER	24.67	74.57	113.72

Taking these values with their known energies (in MeV) we are able to get a relationship between the detector channel number and the corresponding energy. The equations come out as quadratic, and are as follows:

$$\text{UPPER} \quad E = 0.000004427 * C^2 + 0.019403 * C + 0.0416 \quad (4)$$

$$\text{LOWER} \quad E = 0.000004750 * C^2 + 0.018567 * C + 0.0502 \quad (5)$$

Here E is the energy of the disintegration in MeV and C is the channel number on the detector.

If we wish to know the position of a disintegration when given an energy in MeV, we can solve the equations above for C in terms of E:

$$\text{UPPER} \qquad C = -0.55256*E^2 + 51.522*E - 2.125 \tag{6}$$

$$\text{LOWER} \qquad C = -0.66685*E^2 + 53.841*E - 2.673 \tag{7}$$

3.0.0 Data

3.1.0 Explaining the Tables

Tables 3-1 and 3-3 show the counts versus channel numbers for the detectors, with the lower channels along the *horizontal* axis and the upper channels along the *vertical* axis. Similarly, tables 3-2 and 3-4 show the uncertainty in the counts for each respective channel, with the axes labeled in the same way. The uncertainty is calculated by the program written to display the spectrometer run background-subtracted data. The background run was made with all objects in the sample volume except for the meteorite itself.

Tables 3-5 and 3-6 are used in the actual peak determination, and show the summed areas for peak channels with uncertainties factored out. These peak sums are used to determine where the spikes in energy are, and thus can be used to determine the isotope whose decay we are looking at. For a peak channel determination, cells are summed 8 wide by 6 tall to yield a peak-count total given by:

$$x \pm \sqrt{\sum_{i=1}^{n} (\delta x_i^2)} \tag{8}$$

Here 'x' is the sum of an 8x6 cell box, and δx_i is the uncertainty for each cell within the box. For example, the upper and leftmost peak we can observe from using tables 3-1 and 3-2 would be centered at (upper channel) 42.5 x (lower channel) 27.5, as the 8x6 box would be constructed from channel 24 to 31 (lower detector) and 45 to 40 (upper detector). The center of this summed area is then halfway between 24 and 31 for the lower detector and halfway between 45 and 40 on the upper detector, or 27.5 and 42.5, respectively. These peak positions determine the energies of decay in the meteorite sample.

Table 3-7 is a summary of the results which will be discussed in the analysis and conclusion sections of this report. This table shows the identified peaks, corrections to peak channels, energies of those corresponding channels, and difference in MeV of the

experimental results as compared to the disintegration energies we are looking for. The mirrored upper and lower channels have 3 distinct peaks, an issue which will be discussed in the analysis section of this report.

3.2.0 Tables

								Counts (x)								
Position	***24***	***25***	***26***	***27***	***28***	**29**	**30**	**31**	**32**	**33**	**34**	**35**	**36**	**37**	**38**	**39**
45	*0*	*-51*	*14*	*20*	*21*	-1	-4	4	7	17	9	1	-10	-23	-16	7
44	*-8*	*-32*	*-4*	*17*	*32*	-2	-9	-16	30	9	-8	6	10	-4	-9	-13
43	*12*	*-6*	*34*	*-16*	*12*	-7	-2	3	6	-19	5	13	16	-4	-4	-30
42	*43*	*8*	*26*	*-7*	*10*	3	5	5	34	28	22	-7	-4	28	11	-10
41	*21*	*-6*	*44*	*-12*	*-31*	21	34	43	-16	39	28	-5	44	12	-5	-37
40	*-20*	*22*	*43*	*19*	*-16*	16	78	61	36	11	20	28	8	4	-1	-22
39	*9*	*13*	*21*	*44*	*47*	47	61	43	41	53	4	-22	-4	9	30	-21
38	*34*	*12*	*-11*	*1*	*8*	12	32	58	61	42	-29	44	16	13	27	-2
37	*23*	*27*	*-23*	*18*	*-1*	12	44	18	9	48	-5	14	-21	-12	0	18
36	*16*	*-7*	*1*	*13*	*15*	36	10	30	14	54	25	-27	-19	10	30	-3
35	*33*	*42*	*1*	*-5*	*12*	46	27	54	24	31	1	1	4	-8	-11	-17
34	*-29*	*-40*	*-14*	*-22*	*6*	17	2	8	37	-20	7	-4	-7	19	-12	-8
33	*0*	*-8*	*27*	*17*	*-8*	-4	26	22	35	34	-7	16	-27	7	-24	22
32	*44*	*25*	*26*	*-5*	*25*	29	6	25	13	-35	24	10	34	29	51	0
31	*49*	*42*	*24*	*6*	*34*	50	4	45	50	83	61	12	37	73	5	36
30	*55*	*42*	*43*	*9*	*54*	35	33	20	77	41	17	5	31	37	36	99
29	*-6*	*-2*	*-12*	*45*	*40*	58	3	11	19	6	24	-12	24	40	25	30

Table 3-1. Counts vs. Channel

								Uncertainty Counts (±δx)								
Position	***24***	***25***	***26***	***27***	***28***	***29***	***30***	***31***	***32***	***33***	***34***	***35***	***36***	***37***	***38***	***39***
45	*23*	*23*	*24*	*24*	*24*	*23*	*21*	*20*	*18*	*17*	*15*	*15*	*14*	*14*	*14*	*13*
44	*22*	*22*	*23*	*23*	*24*	*23*	*22*	*22*	*21*	*18*	*16*	*16*	*14*	*14*	*14*	*13*
43	*21*	*20*	*22*	*22*	*24*	*24*	*24*	*23*	*22*	*19*	*18*	*16*	*15*	*14*	*14*	*14*
42	*21*	*20*	*21*	*21*	*23*	*24*	*24*	*24*	*24*	*22*	*18*	*17*	*15*	*15*	*15*	*13*
41	*22*	*20*	*21*	*20*	*21*	*23*	*25*	*26*	*25*	*24*	*21*	*19*	*17*	*15*	*14*	*14*
40	*21*	*21*	*20*	*20*	*21*	*23*	*26*	*27*	*26*	*24*	*23*	*21*	*19*	*16*	*16*	*16*
39	*21*	*21*	*21*	*21*	*21*	22	25	26	26	26	24	22	21	18	17	16
38	*21*	*22*	*21*	*21*	*21*	22	24	25	25	25	25	24	22	21	19	16
37	*23*	*23*	*20*	*21*	*20*	22	23	23	24	24	24	24	23	22	20	19
36	*23*	*22*	*21*	*21*	*21*	22	22	22	22	23	23	22	23	22	22	20
35	*23*	*22*	*21*	*21*	*21*	20	21	22	21	21	22	22	22	22	23	21
34	*23*	*23*	*22*	*21*	*21*	21	21	22	22	21	21	20	21	23	22	23
33	*24*	*24*	*23*	*23*	*22*	22	22	22	22	21	21	20	22	23	23	23
32	*26*	*25*	*25*	*24*	*24*	24	24	23	24	22	22	21	22	22	24	25
31	*27*	*27*	*26*	*26*	*25*	24	25	25	24	24	24	22	23	24	25	27
30	*29*	*28*	*28*	*26*	*26*	25	25	25	25	24	23	23	23	23	25	26
29	*27*	*27*	*27*	26	26	25	25	25	24	23	23	22	22	22	22	24

Table 3-2. Uncertainties of Counts

						Counts (x)										
Position	***30***	***31***	***32***	***33***	***34***	***35***	***36***	***37***	***38***	***39***	***40***	***41***	***42***	***43***	***44***	***45***
43	*-2*	*3*	*6*	*-19*	*5*	13	16	-4	-4	-30	29	-4	-12	11	22	21
42	*5*	*5*	*34*	*28*	*22*	-7	-4	28	11	-10	16	-1	-21	-12	21	-14
41	*34*	*43*	*-16*	*39*	*28*	-5	44	12	-5	-37	25	-15	-7	-1	12	0
40	*78*	*61*	*36*	*11*	*20*	28	8	4	-1	-22	-1	0	-7	5	24	-21
39	*61*	*43*	*31*	*53*	*4*	-22	-4	9	30	-21	-9	-22	-6	-28	-16	-19
38	*32*	*58*	*61*	*42*	*-29*	44	16	13	27	-2	17	27	5	10	-16	-15
37	*44*	*18*	*9*	*48*	*-5*	14	-21	-12	0	18	4	-23	-3	17	-11	-2
36	*10*	*30*	*14*	*54*	*25*	-27	-19	10	30	-3	9	1	-31	-6	13	8
35	*27*	*54*	*24*	*31*	*1*	1	4	-8	-11	-17	0	9	1	2	15	-9
34	*2*	*8*	*37*	*-20*	*7*	-4	-7	19	-12	-8	-13	6	7	-5	8	6
33	*26*	*22*	*35*	*34*	*-7*	16	-27	7	-24	22	26	11	-9	17	-32	-3
32	*6*	*25*	*13*	*-35*	*24*	-1	34	29	51	0	27	-15	2	10	1	14
31	*4*	*45*	*50*	*83*	*61*	12	37	73	5	36	35	77	24	38	7	-5
30	*33*	*20*	*77*	*41*	*17*	5	31	37	36	99	56	44	47	44	38	22
29	*3*	*11*	*19*	*6*	*24*	-12	24	40	25	30	29	-4	0	31	45	8
28	*-8*	*38*	*10*	*22*	*8*	4	-8	-18	-6	23	8	-4	-16	2	-5	-13
27	*35*	*-2*	*53*	*27*	*7*	15	7	38	-14	-13	27	30	21	28	-14	-24
26	*58*	*31*	*44*	*7*	*21*	37	15	6	6	41	50	-31	-15	-5	26	-2
25	*49*	*36*	*24*	*23*	*-5*	-119	4	12	51	2	42	16	-9	-3	10	-13
24	36	20	-12	19	17	8	-16	-21	-14	28	13	0	25	-6	14	-8

Table 3-3. Mirror Image Spectra

							Uncertainty Counts (±δx)									
Position	***30***	***31***	***32***	***33***	***34***	***35***	***36***	***37***	***38***	***39***	***40***	***41***	***42***	***43***	***44***	***45***
43	*24*	*23*	*22*	*19*	*18*	16	15	14	14	14	14	13	13	13	13	14
42	*24*	*24*	*24*	*22*	*18*	17	15	15	15	13	14	14	14	13	14	13
41	*25*	*26*	*25*	*24*	*21*	19	17	15	14	14	14	14	13	13	14	13
40	*26*	*27*	*26*	*24*	*23*	21	19	16	16	15	14	14	13	13	13	14
39	*25*	*26*	*26*	*26*	*24*	22	21	18	17	16	14	14	14	14	14	14
38	*24*	*25*	*25*	*25*	*25*	24	22	21	19	16	16	16	15	14	14	14
37	*23*	*23*	*24*	*24*	*24*	24	23	22	20	19	17	16	15	15	14	13
36	*22*	*22*	*22*	*23*	*23*	22	23	22	22	20	18	18	16	15	15	14
35	*21*	*22*	*21*	*21*	*22*	22	22	22	23	21	21	18	17	16	15	14
34	*21*	*22*	*22*	*21*	*21*	20	21	23	22	23	22	21	18	17	15	15
33	*22*	*22*	*22*	*21*	*21*	20	22	23	23	23	23	23	22	20	18	16
32	*24*	*23*	*24*	*22*	*22*	21	22	22	24	25	25	25	24	22	21	20
31	*25*	*25*	*24*	*24*	*24*	22	23	24	25	27	27	28	27	25	24	22
30	*25*	*25*	*25*	*24*	*23*	23	23	23	25	26	27	27	27	26	26	24
29	*25*	*25*	*24*	*23*	*23*	22	22	22	22	24	23	24	25	25	26	25
28	*24*	*24*	*23*	*23*	*22*	21	20	21	21	21	21	22	23	24	24	24
27	*26*	*24*	*24*	*23*	*22*	22	21	20	20	20	21	20	22	23	24	24
26	*27*	*26*	*26*	*24*	*23*	23	22	21	22	22	21	21	21	22	23	24
25	*28*	*27*	*26*	*25*	*24*	23	23	21	22	21	20	21	22	22	22	24
24	*27*	*27*	*27*	*26*	*24*	23	22	21	21	21	21	22	21	21	22	23

Table 3-4. Uncertainty for Mirror Image Spectra

	27.5	28.5	29.5	30.5	31.5	32.5	33.5	34.5	35.5
42.5	265	313	463	385	403	444	434	316	120
41.5	547	619	740	648	618	638	611	473	210
40.5	716	776	885	777	800	848	823	680	354
39.5	805	857	999	937	926	949	896	710	416
38.5	826	886	1069	1035	983	985	879	706	393
37.5	923	1012	1140	1121	1068	986	835	661	355
36.5	649	748	908	934	890	**771**	632	522	282
35.5	436	539	702	712	733	646	556	425	247
34.5	462	508	582	609	603	518	426	345	201
33.5	594	655	750	797	802	740	696	659	505
32.5	765	851	884	882	924	874	858	804	761
31.5	687	807	860	894	874	816	837	844	891

Table 3-5. Center Counts with Uncertainties Factored Out

	33.5	34.5	35.5	36.5	37.5	38.5	39.5	40.5	41.5
40.5	813	670	344	278	118	27	-33	-57	-164
39.5	886	700	406	311	65	-6	-60	-80	-201
38.5	869	696	383	301	29	-55	-83	-94	-174
37.5	825	651	345	196	-44	-94	-125	-94	-162
36.5	622	512	272	108	-97	-121	-131	-100	-156
35.5	556	425	247	113	-42	-60	-64	-27	-65
34.5	416	335	191	113	-9	-84	-46	-12	-37
33.5	686	649	495	405	347	231	290	283	169
32.5	848	794	751	645	642	610	686	653	524
31.5	827	834	881	809	**817**	761	878	853	692
30.5	832	856	904	881	837	756	871	833	688
29.5	905	931	969	929	912	847	974	919	721
28.5	1026	955	1030	982	908	830	905	894	702
27.5	684	615	666	653	579	534	700	725	586
26.5	473	352	333	367	272	207	321	369	257

Table 3-6. Center Counts with Uncertainties Factored Out (Mirrored)

Un-Corrected Peak Channels				**Corrected Peak Channels**	
upper	lower			upper	lower
37.5	29.5			36.929026	29.032834
Un-Corrected Peak Ch. (mirrored)				**Corrected Peak Ch. (mirrored)**	
upper	lower			upper	lower
29.5	39.5			29.007645	39.059354
28.5	33.5			28.016104	33.043442
28.5	35.5			28.016104	35.048746
Energy of Peak Channels (MeV)				**Difference (Accepted-Exp, MeV)**	
upper	lower			upper	lower
0.7641712	0.59326			-0.018821	0.05916357
0.6081604	0.78266			0.0442596	-0.037311783
0.5886712	0.6689			0.0637488	0.076446034
0.5886712	0.70679			0.0637488	0.038564964

Table 3-7. Summary Results Table

4.0.0 Analysis

4.1.0 Visual Aids

Looking at figure 4-1 we see a 3-D representation of a peak which we want to study. The peak is fairly narrow and should be a good candidate to study as there is no plateau feature but rather a "sharp tip" in the peak counts. A sharp peak is important in order to determine the single value which is the energy of the decayed photon as detected by the spectrometer. A wide peak resembling a plateau gives a far worse idea of the center of a peak, and we check our peaks in a 3-D representation in order to visually note the type of peak we are dealing with.

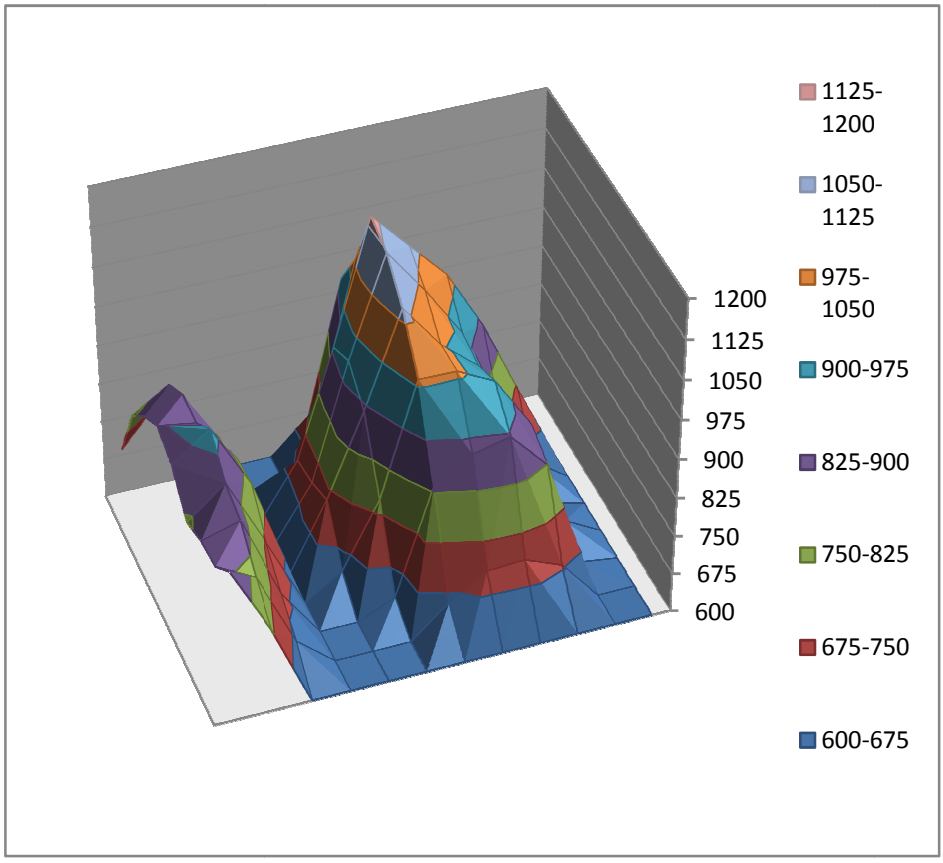

Figure 4-1. 3-D Peak Representation

Figure 4-1 is a 3-D representation of the peak created by use of table 3-5. It doesn't necessarily tell us anything (since channel numbers are not listed, only counts). However, it gives a good idea of the strength of the peak.

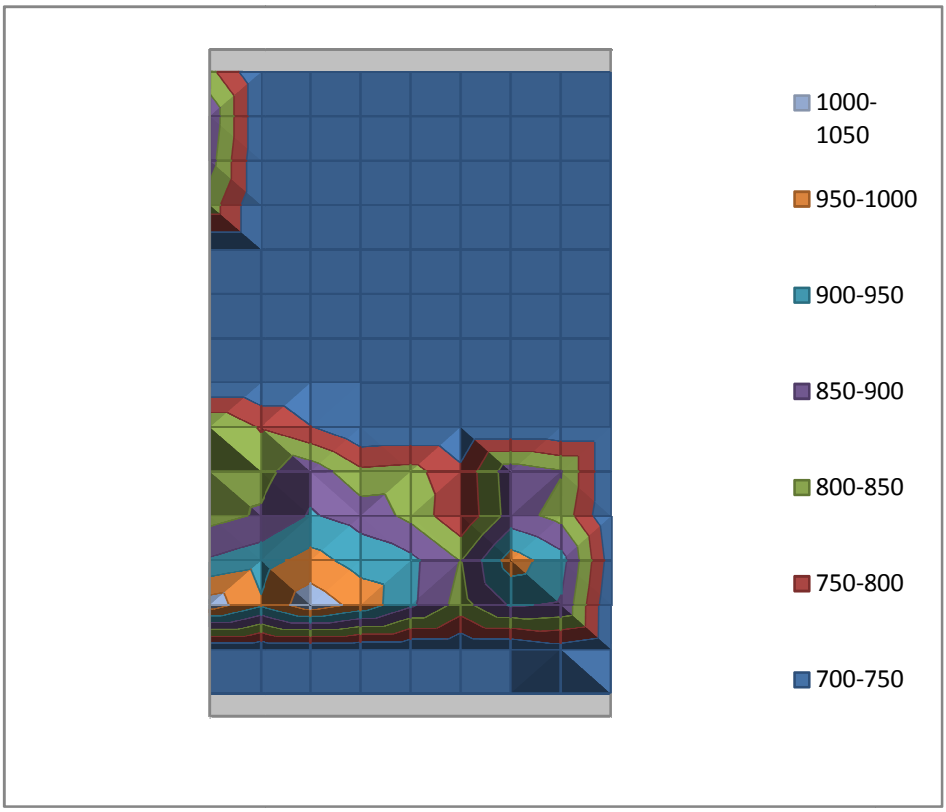

Figure 4-2. 3-D Peak Representation (Mirrored)

Figure 4-2, similarly to figure 4-1, is a 3-D model of the peaks for the mirrored data of table 3-6. This time, the orientation of the view is directly above the peaks (seen in the lower part of the image), and the squares on the image are matched to the cells in table 3-6. Again, this graph is interesting to us only for aesthetic purposes, and doesn't really help in the overall conclusion.

4.2.0 Peak Energies

As noted before, the peak energies which we are interested in finding are 0.6524 MeV and 0.7454 MeV for ^{98}Tc, and would be expected to be found at channels 32.63L x 36.53U and 37.53L x 31.76U, respectively. Looking at table 3-5, we see this 32.63L x 36.53U peak cell in bolded red text, and the location of the largest peak found as the highlighted (in yellow) cell. Similarly, looking at the mirrored table 3-6 we see the 37.53L x 31.76U peak cell in bolded red with other interesting peaks highlighted in yellow.

Though neither of the peaks found perfectly match the expected position for the emitted decay gamma ray, they don't really have to. Uncertainties and drifts in channels can easily shift the peaks of these 0.6524 MeV and 0.7454 MeV gamma rays into slighty different positions, but the more interesting question we need to ask now is what could these peaks be?

Certainly one option is that these peaks are from the decay of ^{98}Tc into ^{98}Ru as seen in figure 1-1, as they are in coincidence (as expected) and near the right energy values. Other possibilities for decays which will need to be ruled out before a final decision is made can be found through a search of the National Nuclear Data Center online (http://www.nndc.bnl.gov). Two other elements with similar energies of decay are ^{166}Ho, which has disintegration energies at: 611, 670, 691, 711, 752, 778, 810, and 830 (all energies in keV), and also ^{108}Ag with disintegration energies at: 614 keV and 723 MeV.

4.3.0 Conversion of Peaks Found to MeV

Looking at tables 3-5 and 3-6, the strongest peak(s) are highlighted around the region where we expect to find the 0.6524 MeV and 0.7454 MeV peaks from the disintegration of the ^{98}Tc into ^{98}Ru. Starting with the peak highlighted in table 3-5 and seen in figure 4-1, equations 4 and 5 are used to convert the upper and lower channel numbers into energies of disintegration:

UPPER $E_U = 0.76417$ MeV

LOWER $E_L = 0.59326$ MeV

Then with table 3-6, we examine the highlighted peaks seen in figure 4-2 using equations 4 and 5 in a similar fashion:

UPPER $E_U = 0.60816$ MeV

LOWER $E_L = 0.78266$ MeV

UPPER $E_U = 0.58867$ MeV

LOWER $E_L = 0.66890$ MeV

UPPER $E_U = 0.58867$ MeV

LOWER $E_L = 0.70679$ MeV

In the above list, the red-colored values indicate the closest values to the energies of ^{98}Tc, which are 6.78% and 5.01% different (upper and lower).

5.0.0 Conclusion

The main goal behind this study was to learn the methods by which spectroscopy is conducted, as well as to attempt to detect the isotope ^{98}Tc in a meteorite sample, and thus find evidence of ^{98}Tc from a source other than spectral lines from distant stars. The proximity of the peaks found to the position of peaks predicted from the disintegration energies for ^{98}Tc (0.6524 MeV and 0.7454 MeV) make the possibility of having found ^{98}Tc in the Lake Labyrinth meteorite sample realistic.

The results to date (seen in summary table 5-1) indicate that there is a reasonable possibility that I have found ^{98}Tc gamma rays coming from the Lake Labyrinth meteorite. However, further studies are needed to confirm that the gamma-ray energies coming from that meteorite do have exactly the correct values for ^{98}Tc disintegrations, and that these gamma-ray energies do not originate from disintegrations from any other isotope.

Energy of Peak Channels (MeV)				**Difference (Accepted-Exp, MeV)**			**% Difference**	
upper	lower			upper	lower		upper	lower
0.76417	0.59326			-0.01882	0.05916		2.53	9.07
0.60816	0.78266			0.04426	-0.03731		6.78	5.01
0.58867	0.66890			0.06375	0.07645		9.77	10.3
0.58867	0.70679			0.06375	0.03856		9.77	5.17

Table 5-1. Peak Energies Summary

6.0.0 Bibliography

Thomas Jefferson National Accelerator Facility - Office of Science Education. "It's Elemental - The Element Technetium." *Science Education at Jefferson Lab*. Web. 05 Jan. 2010. <http://education.jlab.org/itselemental/ele043.html>.

NNDC. National Nuclear Data Center, May 2003. Web. 5 Jan. 2010. <http://www.nndc.bnl.gov/cgi-bin/mirdtab.cgi>.

Ginn, Aaron S. "Gamma Ray Spectroscopy of Meteorite Samples with Attention to Assay of ^{26}Al." Senior Project Report. California Polytechnic University: San Luis Obispo, 1993. Print.

Malaney, Robert A. "Production of technetium in red giants by gamma-ray-induced fission." *Nature* 337 (1989): 718-19. Print.